Search for $\bar{\nu}_e$ from the Sun at Super-Kamiokande-I

Y. Gando,[24] S. Fukuda,[1] Y. Fukuda,[1] M. Ishitsuka,[1] Y. Itow,[1] T. Kajita,[1] J. Kameda,[1,9] K. Kaneyuki,[1] K. Kobayashi,[1] Y. Koshio,[1] M. Miura,[1] S. Moriyama,[1] M. Nakahata,[1] S. Nakayama,[1] T. Namba,[1] Y. Obayashi,[1] A. Okada,[1] T. Ooyabu,[1] C. Saji,[1] N. Sakurai,[1] M. Shiozawa,[1] Y. Suzuki,[1] H. Takeuchi,[1] Y. Takeuchi,[1] Y. Totsuka,[1,9] S. Yamada,[1] S. Desai,[2] M. Earl,[2] E. Kearns,[2] M. D. Messier,[2,*] J. L. Stone,[2] L. R. Sulak,[2] C.W. Walter,[2] M. Goldhaber,[3] T. Barszczak,[4] D. Casper,[4] W. Gajewski,[4] W. R. Kropp,[4] S. Mine,[4] D.W. Liu,[4] M. B. Smy,[4] H.W. Sobel,[4] M. R. Vagins,[4] A. Gago,[5] K. S. Ganezer,[5] J. Hill,[5] W. E. Keig,[5] R.W. Ellsworth,[6] S. Tasaka,[7] A. Kibayashi,[8] J. G. Learned,[8] S. Matsuno,[8] D. Takemori,[8] Y. Hayato,[9] A. K. Ichikawa,[9] T. Ishii,[9] T. Kobayashi,[9] T. Maruyama,[9,†] K. Nakamura,[9] Y. Oyama,[9] M. Sakuda,[9] M. Yoshida,[9] M. Kohama,[10,‡] T. Iwashita,[10] A. T. Suzuki,[10] T. Inagaki,[11] I. Kato,[11] T. Nakaya,[11] K. Nishikawa,[11] T. J. Haines,[12,4] S. Dazeley,[13] S. Hatakeyama,[13] R. Svoboda,[13] E. Blaufuss,[14] M. L. Chen,[14] J. A. Goodman,[14] G. Guillian,[14] G.W. Sullivan,[14] D. Turcan,[14] K. Scholberg,[15] A. Habig,[16] M. Ackermann,[17] C. K. Jung,[17] K. Martens,[17,§] M. Malek,[17] C. Mauger,[17] C. McGrew,[17] E. Sharkey,[17] B. Viren,[17,3] C. Yanagisawa,[17] T. Toshito,[18] C. Mitsuda,[19] K. Miyano,[19] T. Shibata,[19] Y. Kajiyama,[20] Y. Nagashima,[20] K. Nitta,[20] M. Takita,[20] H. I. Kim,[21] S. B. Kim,[21] J. Yoo,[21] H. Okazawa,[22] T. Ishizuka,[23] M. Etoh,[24] T. Hasegawa,[24] K. Inoue,[24] K. Ishihara,[24] J. Shirai,[24] A. Suzuki,[24] M. Koshiba,[25] Y. Hatakeyama,[26] Y. Ichikawa,[26] M. Koike,[26] K. Nishijima,[26] H. Ishino,[27] M. Morii,[27] R. Nishimura,[27] Y. Watanabe,[27] D. Kielczewska,[28,4] H. G. Berns,[29] S. C. Boyd,[29] A. L. Stachyra,[29] and R. J. Wilkes[29]

(Super-Kamiokande Collaboration)

[1]*Institute for Cosmic Ray Research, University of Tokyo, Kashiwa, Chiba 277-8582, Japan*
[2]*Department of Physics, Boston University, Boston, Massachusetts 02215, USA*
[3]*Physics Department, Brookhaven National Laboratory, Upton, New York 11973, USA*
[4]*Department of Physics and Astronomy, University of California, Irvine, Irvine, California 92697-4575, USA*
[5]*Department of Physics, California State University, Dominguez Hills, Carson, California 90747, USA*
[6]*Department of Physics, George Mason University, Fairfax, Virginia 22030, USA*
[7]*Department of Physics, Gifu University, Gifu, Gifu 501-1193, Japan*
[8]*Department of Physics and Astronomy, University of Hawaii, Honolulu, Hawaii 96822, USA*
[9]*Institute of Particle and Nuclear Studies, High Energy Accelerator Research Organization (KEK), Tsukuba, Ibaraki 305-0801, Japan*
[10]*Department of Physics, Kobe University, Kobe, Hyogo 657-8501, Japan*
[11]*Department of Physics, Kyoto University, Kyoto 606-8502, Japan*
[12]*Physics Division, P-23, Los Alamos National Laboratory, Los Alamos, New Mexico 87544, USA*
[13]*Department of Physics and Astronomy, Louisiana State University, Baton Rouge, Louisiana 70803, USA*
[14]*Department of Physics, University of Maryland, College Park, Maryland 20742, USA*
[15]*Department of Physics, Massachusetts Institute of Technology, Cambridge, Massachusetts 02139, USA*
[16]*Department of Physics, University of Minnesota, Duluth, Minnesota 55812-2496, USA*
[17]*Department of Physics and Astronomy, State University of New York, Stony Brook, New York 11794-3800, USA*
[18]*Department of Physics, Nagoya University, Nagoya, Aichi 464-8602, Japan*
[19]*Department of Physics, Niigata University, Niigata, Niigata 950-2181, Japan*
[20]*Department of Physics, Osaka University, Toyonaka, Osaka 560-0043, Japan*
[21]*Department of Physics, Seoul National University, Seoul 151-742, Korea*
[22]*Internatinal and Cultural Studies, Shizuoka Seika College, Yaizu, Shizuoka, 425-8611, Japan*
[23]*Department of Systems Engineering, Shizuoka University, Hamamatsu, Shizuoka 432-8561, Japan*
[24]*Research Center for Neutrino Science, Tohoku University, Sendai, Miyagi 980-8578, Japan*
[25]*The University of Tokyo, Tokyo 113-0033, Japan*
[26]*Department of Physics, Tokai University, Hiratsuka, Kanagawa 259-1292, Japan*
[27]*Department of Physics, Tokyo Institute for Technology, Meguro, Tokyo 152-8551, Japan*
[28]*Institute of Experimental Physics, Warsaw University, 00-681 Warsaw, Poland*
[29]*Department of Physics, University of Washington, Seattle, Washington 98195-1560, USA*
(Received 30 December 2002; published 1 May 2003)

We present the results of a search for low energy $\bar{\nu}_e$ from the Sun using 1496 days of data from Super-Kamiokande-I. We observe no significant excess of events and set an upper limit for the conversion probability to $\bar{\nu}_e$ of the ^{8}B solar neutrino. This conversion limit is 0.8% (90% C.L.) of the standard solar

 0031-9007/03/90(17)/171302(5)$20.00

model's neutrino flux for total energy = 8–20 MeV. We also set a flux limit for monochromatic $\bar{\nu}_e$ for $E_{\bar{\nu}_e} = 10$–17 MeV.

DOI: 10.1103/PhysRevLett.90.171302 PACS numbers: 26.65.+t, 14.60.Pq, 95.85.Ry, 96.40.Tv

Solar neutrino measurements at Super-Kamiokande [1] and Sudbury Neutrino Observatory (SNO) [2] have established that the solar neutrino problem is explained by the transformation of electron neutrinos to other active neutrinos. The mechanism for this transformation is generally assumed to be via neutrino flavor oscillations from ν_e to some superposition of ν_μ and ν_τ. However, measurements reported thus far do not rule out the possibility of spin flavor precession (SFP) in which some of the ν_e transform to antiparticles ($\bar{\nu}_\mu$, $\bar{\nu}_\tau$). In the so-called "hybrid models" [3], SFP and oscillation can transform solar neutrinos to $\bar{\nu}_e$ if the neutrino is Majorana, it has a large magnetic moment, and the Sun has a large magnetic field. If the neutrino has a magnetic moment, there are two possibilities: (1) The neutrino is a Dirac particle; (2) it is a Majorana particle. In the Dirac neutrino case, ν_e^L changes to ν_e^R by the spin magnetic moment transition. The ν_e^R is a sterile neutrino. On the other hand, in the Majorana neutrino scenario, SFP causes $\nu_e \rightarrow \bar{\nu}_{\mu,\tau}$. Neutrino oscillation then yields $\bar{\nu}_{\mu,\tau} \rightarrow \bar{\nu}_e$. Solar $\bar{\nu}_e$ could also originate from neutrino decay [4]. In this paper, we present a search for $\bar{\nu}_e$ from the Sun.

The inverse beta decay process, $\bar{\nu}_e + p \rightarrow n + e^+$, is predominant for $\bar{\nu}_e$ interactions in Super-Kamiokande (SK). The cross section for this process is 2 orders of magnitude greater than that for elastic scattering, and therefore SK has good sensitivity for the detection of solar $\bar{\nu}_e$. The positron energy is related to the neutrino energy by $E_{e^+} \approx E_{\bar{\nu}_e} - 1.3$ MeV. The positron angular distribution relative to the incident $\bar{\nu}_e$ direction is nearly flat with a small energy dependent slope [5], which is in contrast to the sharply forward peaked elastic scattering distribution. The difference between these distributions can be used to separate solar neutrino events from $\bar{\nu}_e$ events.

Super-Kamiokande is a 22.5 kton fiducial volume water Cherenkov detector, located in the Kamioka mine in Gifu, Japan. The data used for the search were collected in 1496 live days between 31 May 1996 and 15 July 2001. A detailed description of SK can be found elsewhere [1,6]. Dominant backgrounds to the solar neutrino signal are ^{222}Rn in the water, external gamma rays, and muon-induced spallation products. Background reduction is carried out in the following steps: first reduction, spallation cut, second reduction, and external γ-ray cut. The first reduction removes events from electronic noise and other nonphysical sources, and events with poorly reconstructed vertices. The spallation cut removes events due to radioisotopes (X) produced by cosmic ray muon interactions with water: $\mu + {}^{16}\mathrm{O} \rightarrow \mu + X$. These radioisotopes are called "spallation products." The spallation products emit beta and gamma rays and have lifetimes ranging from 0.001 to 14 sec. We cut these events using likelihood functions based on time, position, and muon pulse height. The time and position likelihood functions are measures of the proximity of a candidate event to a muon track, while the pulse height likelihood function measures the likelihood that a muon produced a shower. These three likelihood functions are used together to discriminate against spallation events [6]. The second reduction removes events with poor vertex fit quality and diffuse Cherenkov ring patterns, both characteristics of low-energy background events. The external γ-ray cut removes events due to γ rays from the surrounding rock, photomultipliers (PMTs), etc. Figure. 1 shows the energy spectrum after each reduction step.

At SK, a positron from inverse beta decay is indistinguishable from an electron or a gamma ray because the delayed 2.2 MeV gamma ray from $n + p \rightarrow d + \gamma$ is below the detector's energy threshold. In order to remove elastic scattering events due to solar neutrinos, we cut events with $\cos\theta_{\rm sun} \geq 0.5$, where $\theta_{\rm sun}$ is the event direction with respect to the direction from the Sun. The region $\cos\theta_{\rm sun} < 0.5$ would be occupied by solar $\bar{\nu}_e$ events, in addition to events due to known background sources which could not be removed by the standard data reduction. For $E \lesssim 8$ MeV, most background events are due to radioactivity in the detector materials (such as ^{222}Rn). Spallation accounts for a small fraction of

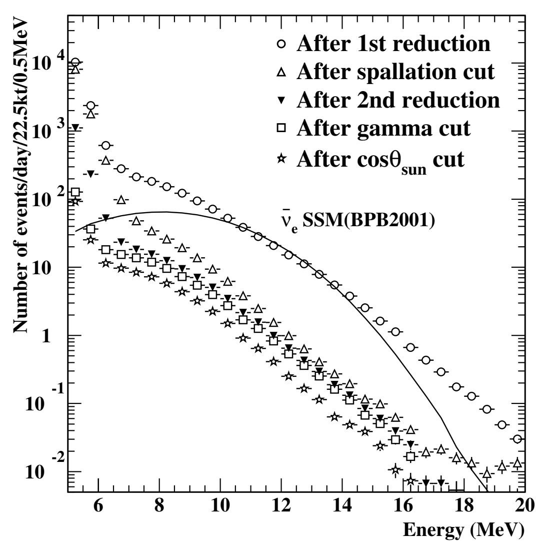

FIG. 1. Energy spectrum after each reduction step. The solid curve shows the expected positron spectrum, after all cuts, assuming all ^{8}B solar neutrinos convert to $\bar{\nu}_e$. The horizontal axis shows the reconstructed total $e^{\pm}$ energy.

background events in this region. In contrast, for $E \gtrsim 8$ MeV, most background events are produced by spallation.

The spallation cut used in the data reduction efficiently removes short-lifetime spallation products. This cut also removes ~90% of long-lifetime products such as ${}^{16}_{7}$N ($\tau_{1/2} = 7.1$ sec) and ${}^{11}_{4}$Be ($\tau_{1/2} = 13.8$ sec). Event by event removal of the remaining ~10% of these events is impractical because this introduces large dead time. However, we can estimate the contribution of these events to the postreduction data sample using a statistical subtraction technique. First, we made a time distribution of muon events preceding each low energy event by up to 200 sec [Fig. 2(A)]. Since the average muon rate at SK is ≈2.5 Hz, there are, on average, ≈500 events for each low energy event. If the low energy event is due to a long lifetime spallation product, its event time will be correlated with one of the ~500 preceding muon events. If this is not the case, then its event time will be uncorrelated with all of the muon events. To estimate the number of μ responsible for spallation events, we have to subtract the number of μ which did not make spallation events from the total number of μ. In order to perform this subtraction, we made a sample of simulated events distributed randomly in space and time. We applied the spallation cut to this sample as in the actual data sample in order to account for biases introduced by this cut. The muon time distribution of the random sample is shown in Fig. 2(B). The dip near delta-T = 0 is due to the accidental loss of events by the spallation cut. To estimate the number of muons which made spallation products, distribution 2(B) with suitable normalization is subtracted from distribution 2(A); the result of this subtraction is shown in Fig. 2(C). The number of muon events in the delta-T = 100–200 sec region is used to calculate the normalization factor because the contamination from muons which make spallation products is negligible in this region. The number of spallation events is obtained as

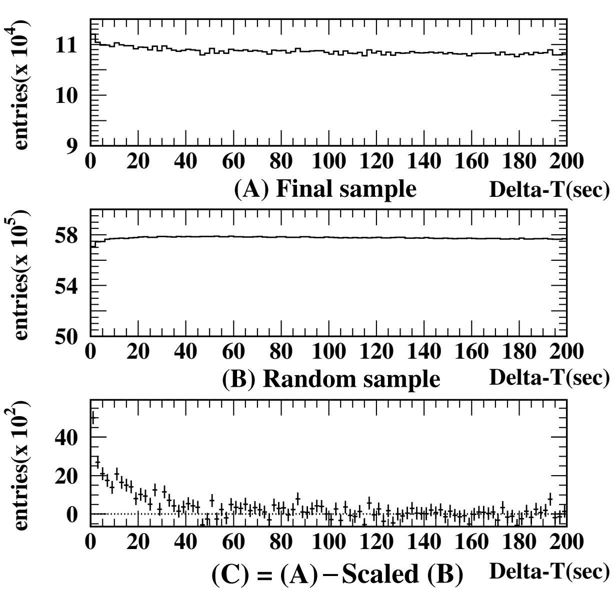

FIG. 2. (A) μ delta-T distribution before observed events. (B) Before random events. (C) The delta-T distribution of events caused by spallation products obtained as (A) − scale factor × (B).

$$\mathrm{Spa} = N^{\mathrm{observed}}_{0\text{--}50\,\mathrm{sec}} - N^{\mathrm{random}}_{0\text{--}50\,\mathrm{sec}} \times \frac{N^{\mathrm{observed}}_{100\text{--}200\,\mathrm{sec}}}{N^{\mathrm{random}}_{100\text{--}200\,\mathrm{sec}}}.$$

$N^{\mathrm{observed}}_{0\text{--}50\,\mathrm{sec}}$ is the number of muon events within 50 sec preceding the observed events, while $N^{\mathrm{random}}_{0\text{--}50\,\mathrm{sec}}$ is the corresponding number for random events. $N^{\mathrm{observed}}_{100\text{--}200\,\mathrm{sec}}$ and $N^{\mathrm{random}}_{100\text{--}200\,\mathrm{sec}}$ are similarly defined, but with a timing window of 100 to 200 sec preceding the events. For 8.0–20.0 MeV, and $\cos\theta_{\mathrm{sun}} \leq 0.5$, the number of spallation background events obtained by this method is $(2.77 \pm 0.20) \times 10^4$. The number of observed $\bar{\nu}_e$ candidate events is 29 781, so the ratio of spallation events to observed events is $(93 \pm 7)\%$. The spallation contamination in each energy bin is shown in Fig. 3.

The energy spectrum of the solar $\bar{\nu}_e$ is not known because the mechanism for $\bar{\nu}_e$ creation is not known. Even if one assumes the SFP-oscillation hybrid model, the energy spectrum depends on $\mu_\nu \times B_{\mathrm{solar}}$, Δm^2, and $\sin^2(2\theta)$, none of which are known precisely, if at all. In order to deal with this ambiguity, we have chosen two spectrum models: the ^{8}B neutrino spectrum [7] and monochromatic spectrum (spectrum independent analysis).

For the ^{8}B spectrum dependent analysis, we obtain an upper limit on the solar $\bar{\nu}_e$ flux by comparing the observed number of events outside of the elastic scattering peak ($\cos\theta_{\mathrm{sun}} \leq 0.5$) with the expected number of $\bar{\nu}_e$

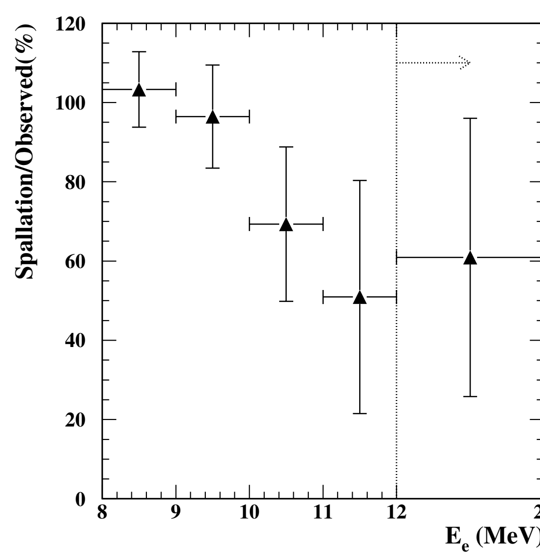

FIG. 3. Spallation contamination in each energy bin. The horizontal axis shows the total energy and the vertical axis shows the ratio of spallation events to observed events.

events assuming that all ^{8}B neutrinos convert to $\bar{\nu}_e$. The expected number is obtained by Monte Carlo simulation of solar $\bar{\nu}_e$ interaction with the detector. The $\cos\theta_{\rm sun}$ dependence was simulated, and the effect of this dependence on the $\bar{\nu}_e$ efficiency is taken into account. The standard solar model (SSM) ^{8}B neutrino flux was assumed ($5.05 \times 10^6/\mathrm{cm}^2/\mathrm{sec}$) [8]. Through the rest of this paper, electron neutrino spectrum and flux refer to the unoscillated quantities at the Sun. The solid lines in Fig. 4 show 90% C.L. limits on the $\bar{\nu}_e$ flux before statistical spallation subtraction. The dashed lines show the limits after statistical subtraction (only for $E \geq 8$ MeV). By combining the statistics for 8 MeV $\leq E \leq$ 20 MeV, we obtained a global upper limit of 0.8% of the SSM neutrino flux.

Some authors have indicated that the positron angular distribution may be useful for the search for $\bar{\nu}_e$ in the SK data (e.g., [9,10]). $\cos\theta_{\rm sun}$ is distributed as $f(\cos\theta_{\rm sun}) = 0.5 \times (1 + \alpha \times \cos\theta_{\rm sun})$, where α is a monotonically increasing function of neutrino energy (except near threshold), and $\alpha < 0$ for $E_\nu \lesssim 13$ MeV and > 0 above this [5]. The angular information is useful for the $\bar{\nu}_e$ search at the lowest neutrino energies where $f(\cos\theta_{\rm sun})$ has sufficient slope and the event statistics are large. $\bar{\nu}_e$ events with the predicted $\cos\theta_{\rm sun}$ distribution were input to a detector simulator to obtain the expected positron angular distribution. The resulting distribution has the same form as above. The fit value of α is -0.076 at $E = 5$–6 MeV, 0.107 at $E = 12$–20 MeV, and crosses 0 at ~9 MeV.

Solar neutrino elastic scattering is one of the backgrounds for this analysis. Almost all such events have $\cos\theta_{\rm sun} > 0.5$, so events with $\cos\theta_{\rm sun} > 0.5$ are cut. We also subtract the small amount of spillover into $\cos\theta_{\rm sun} \leq 0.5$ using Monte Carlo simulation (~5% for 5–20 MeV). Another background is due to $^{18}\mathrm{O}(\nu_e; e)^{18}\mathrm{F}$ [11]. There is only a small number of events from this source (~ 0.03%–2%, depending on energy), but electrons from this process, such as the low-energy $\bar{\nu}_e$, have negative slope in their angular distribution, so they are subtracted from the data. The ν_e flux is taken as the charged current flux value from SNO, $1.76 \times 10^6/\mathrm{cm}^2/\mathrm{sec}$ [12].

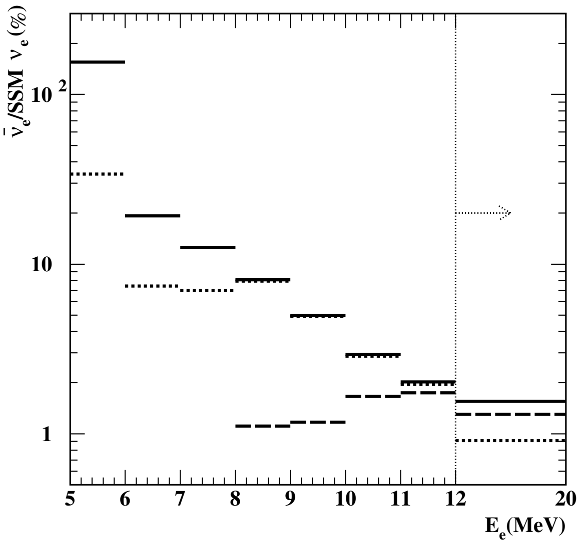

FIG. 4. Summary of $\bar{\nu}_e$ limits. The horizontal axis shows total positron energy and the vertical axis shows the 90% C.L. $\bar{\nu}_e$ rate normalized to the SSM ν_e rate. The solid lines show the 90% C.L. limit ratio. The dashed lines show the limit after statistical subtraction of the spallation background. The dotted lines show the result from the angular distribution analysis.

A $\bar{\nu}_e$ flux upper limit is obtained using a probability test with the slope of the $\cos\theta_{\rm sun}$ distribution serving as a constraint. This test is based on a χ^2 test with $\chi^2(\delta, \beta, \gamma)$ defined for each energy as follows:

$$\sum_{i=1}^{N_{\cos}} \left\{ \frac{N_i^{\rm data} - N_i^{el} - N_i^{^{18}\mathrm{O}} - \delta \cdot N_i^{\bar{\nu}_e} - \beta \cdot n_i^{\rm BG}(1 + \gamma \cdot x_i)}{\sigma_i^{\rm stat}} \right\}^2 + \left(\frac{\gamma}{\sigma^{\rm syst}} \right)^2.$$

i is the index for the $\cos\theta_{\rm sun}$ bins ($\cos\theta_{\rm sun} \leq 0.5$, $N_{\cos} = 30$), x_i is $(\cos\theta_{\rm sun})_i$, $N_i^{\rm data}$ is the number of observed data events, $\sigma_i^{\rm stat}$ is the statistical error of the observed data, N_i^{el} is the expected number of elastic scattering events, $N_i^{^{18}\mathrm{O}}$ is the expected number of events from the $^{18}\mathrm{O}(\nu_e; e)^{18}\mathrm{F}$ reaction, $N_i^{\bar{\nu}_e}$ is the number of $\bar{\nu}_e$ events assuming all SSM ν_e convert to $\bar{\nu}_e$ (the number in each bin i depends on the slope α), and $n_i^{\rm BG}$ is the shape for all other background events that are almost uncorrelated in direction with the Sun (this background is essentially flat). N_i^{el} and $N_i^{^{18}\mathrm{O}}$ are both $\lesssim 2\%$ of $N_i^{\rm data}$, and the systematic errors of these terms are negligible. $\sigma^{\rm syst}(= 0.5\%)$ is the systematic error of the slope of the background shape and γ is the parameter that takes this into account. β parametrizes the amount of such background events. We divided the parameter space for δ into a grid, and minimized χ^2 with respect to β and γ at each grid point. The resulting γ and $\chi^2_{\rm min}$ indicated good fits to the data. χ^2 as a function δ obtained in this way is input to a probability function. From this analysis, we set a 90% C.L. upper limit for each energy bin. The dotted lines in Fig. 4 show the result. It should be noted that the spallation background subtraction is not applied in this analysis for two reasons. First, for $E < 8$ MeV, spallation subtraction is ineffective because spallation events form a small subset of the total background. Second, for $E > 8$ MeV, there are insufficient statistics after spallation subtraction to perform an angular analysis of the data.

The analysis described thus far assume that the $\bar{\nu}_e$ originate from ^{8}B solar neutrinos. We also generalized our search by assuming a monochromatic $\bar{\nu}_e$ source at

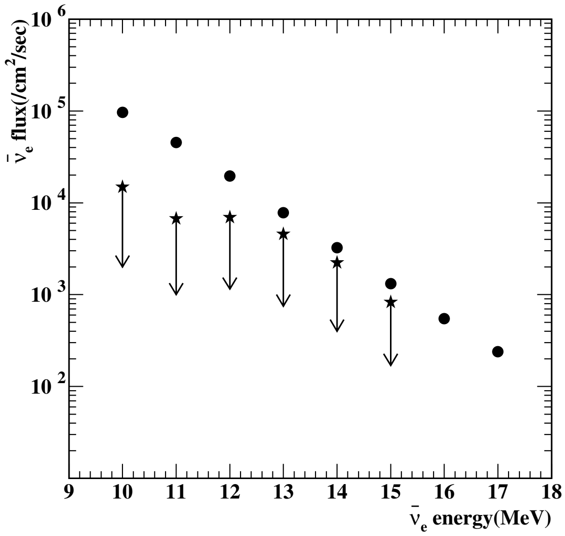

FIG. 5. $\bar{\nu}_e$ flux 90% C.L. upper limit for each monochromatic $\bar{\nu}_e$. The horizontal axis shows neutrino energy and the vertical axis shows the flux limit. The circles show the limits before spallation subtraction while the stars show the limits after subtraction. The two highest-energy bins have an insufficient number of events for statistical subtraction.

various energies and set conservative $\bar{\nu}_e$ flux upper limits. The interaction of such $\bar{\nu}_e$ with the detector was simulated, and standard data reduction cuts were applied. The positron spectrum is well described by a Gaussian. We then counted the number of events in the data in the $\pm 1\sigma$ range of this Gaussian. We took this number to be the number of events due to monochromatic $\bar{\nu}_e$ and obtained an upper limit. This upper limit is very conservative because we do not take account of the large spillover from lower energy bins that is implied by the sharply falling spectrum seen in the data. We also obtained limits after statistical subtraction of long lifetime spallation events. The 90% C.L. limits are shown in Fig. 5.

In summary, a search for $\bar{\nu}_e$ flux from the Sun was performed using all 1496 live days of solar neutrino data from Super-Kamiokande-I. Using the ^{8}B and monochromatic energy spectra, 90% C.L. upper limits were set for the $\bar{\nu}_e$ flux. For the ^{8}B spectrum dependent analysis, the upper limit to the flux was 0.8% of the SSM ν_e flux prediction for $E = 8.0$–20.0 MeV. This can be compared with the Kamiokande result of 4.5% [13]. For $\bar{\nu}_e$ fluxes with various monochromatic energies, the resulting upper limits are shown in Fig. 5.

The authors acknowledge the cooperation of the Kamioka Mining and Smelting Company. The Super-Kamiokande has been built and operated from funding by the Japanese Ministry of Education, Culture, Sports, Science and Technology, the U.S. Department of Energy, and the U.S. National Science Foundation. This work was partially supported by the Korean Research Foundation (BK21) and the Korea Ministry of Science and Technology.

*Present address: Harvard University, Cambridge, MA 02138, USA.
†Present address: Enrico Fermi Institute, University of Chicago, Chicago, IL 60637, USA.
‡Present address: The Institute of Physical and Chemical Reasearch (RIKEN), Wako, Saitama 351-0198, Japan.
§Present address: Department of Physics, University of Utah, Salt Lake City, UT 84112, USA.

[1] S. Fukuda *et al.*, Phys. Lett. B **539**, 179 (2002).
[2] Q. R. Ahmad *et al.*, Phys. Rev. Lett. **87**, 071301 (2001)
[3] C. S. Lim and W. J. Marciano, Phys. Rev. D **37**, 1368 (1988); E. Kh. Akhmedov, Phys. Lett. B **213**, 64 (1988); Sov. Phys. JETP **68**, 690 (1989).J. Barranco *et al.*, Phys. Rev. D **66**, 093009 (2003).
[4] Z. Berezhiani, G. Fiorentini, M. Moretti, and A. Rossi, JETP Lett. **55**, 151 (1992); A. Acker, A. Joshipura, and S. Pakvasa, Phys. Lett. B **285**, 371 (1992); R. S. Raghavan, X.-G. He, and S. Pakvasa, Phys. Rev. D **38**, 1317 (1988); J. F. Beacom and N. F. Bell, Phys. Rev. D **65**, 113009 (2002).
[5] P. Vogel and J. F. Beacom, Phys. Rev. D **60**, 053003 (1999).
[6] Y. Fukuda *et al.*, Phys. Rev. Lett. **81**, 1158 (1998); M. Nakahata *et al.*, Nucl. Instrum. Methods Phys. Res., Sect. A **421**, 113 (1999).Y. Fukuda *et al.*, Phys. Rev. Lett. **82**, 2430 (1999).Y. Fukuda *et al.*, Phys. Rev. Lett. **82**, 1810 (1999); S. Fukuda *et al.*, Phys. Rev. Lett. **86**, 5651 (2001).
[7] C. E. Ortiz *et al.*, Phys. Rev. Lett. 85, 2909 (2000).
[8] J. N. Bahcall *et al.*, Astrophys. J. **555**, 990 (2001).
[9] G. Fiorentini, M. Moretti, and F. L. Villante, Phys. Lett. B **413**, 378 (1997).
[10] E. Torrente-Lujan, Phys. Lett. B **494**, 255 (2000).
[11] W. C. Haxton and R. G. H. Robertson, Phys. Rev. C **59**, 515 (1999).
[12] Q. R. Ahmad *et al.*, Phys. Rev. Lett. **89**, 011301 (2002).
[13] K. Inoue, Ph.D. thesis, University of Tokyo, 1993.